Journal of Computers Vol. 34 No. 3, June 2023, pp. 151-164
doi: 10.53106/199115992023063403011

A Recognition Method of Ceramic Microcosmic Images Based on SURF and Blockchain

You-Dong Wang[1], Xing Xu[2*], Xi-En Cheng[3]

[1] School of Computer Science, Minnan Normal University,
Zhangzhou 363000, China
wangyoumudong@163.com

[2] School of Physics and Information Engineering, Minnan Normal University,
Zhangzhou 363000, China
xx1889@mnnu.edu.cn

[3] School of Information Engineering, Jingdezhen Ceramic Institute,
Jingdezhen 333000, China
9567113@qq.com

Received 28 June 2022; Revised 4 October 2022; Accepted 11 December 2022

Abstract. Ceramics have gradually occupied a more significant proportion in the art market and daily life in recent years. Therefore, the identification and anti-counterfeiting of ceramics have become more important with the continuous improvement of counterfeit ceramics. However, it is difficult for traditional ceramic identification and anti-counterfeiting technology to make instant, accurate and efficient identifications. Hence, based on the speed-ed up robust feature (SURF) algorithm, this paper proposes to take the microscopic surface features of ceramic images as the unique identifier for ceramic. In addition, blockchain was combined with distributed storage to ensure the security and reliability of these micro-characteristic data. At any time, ceramic images to be identified can be compared and verified with these images stored on the blockchain, and hence to determine the authenticity of the ceramics. Experimental results show that the proposed method has a high recognition rate and good robustness to problems. Compared with the traditional feature extraction methods, the efficiency and accuracy of proposed algorithm have been improved. The matching similarity rate between most imitations and genuine products using the proposed algorithm will not exceed 15%, thus accurately identifying imitations to achieve the anti-counterfeiting of ceramics.

Keywords: ceramics identification, anti-counterfeiting, microcosmic features, SURF, blockchain

1 Introduction

Nowadays, ceramics have gradually become popular because of their outstanding artistry and collection value. Besides the artistic ceramics which are worth collecting, daily ceramics produced by high-end ceramic brands have also occupied a large proportion of the art market. With the continuous development of the market and the continuous improvement of counterfeiting, more highly-imitated counterfeit ceramic art products continue to be made, which disrupts the normal art ceramic market and seriously threatens the sustainable development of the art ceramic market.

In the past, macro parameters such as shape, size, and weight were used to determine the "identification" of ceramics. However, it is increasingly challenging for traditional identification methods to identify ceramic fakes which have been constantly refined. Therefore, it is significant to find a more convenient and efficient method of ceramic identification and comparative traceability to examine the art ceramics.

At present, the traditional method of identifying ceramics can be roughly divided into two types. The first type is the visual identification method, in which the ceramics type, tire glaze, ornamentation, style recognition, craftsmanship [1], and other aspects have been used for the identification. Nevertheless, only a few experienced experts can provide identification and conclusions through visual and tactile sense and combine the authentication with their own experience in ceramic identification. Moreover, due to the high value of some art porcelains, manual identification does not have such credibility that everyone can believe in. The second type is the

* Corresponding Author

technological identification methods combined with computer science [2]. With the advancement of science and technology, combining computers with ceramic identification is more reliable and reasonable for the business environment. In the past, people commonly used labels to store ceramic information for identification. For example, bar codes technology and QR codes technology are common ways to identify products in life. However, it is not so difficult to make such codes that there is an excellent possibility of replicability. Therefore, more and more application scenarios are now considering using radio frequency identification (RFID) tags [3] for identification. For example, Babar and others have presented a small and flexible metal mountable UHF RFID tag antenna [4]. However, whether bar code or electronic label may leave traces on the surface of ceramics. These traces not only destroy its integrity and affect its beauty but also greatly damage its artistic value and collection value for precious ceramic art.

Therefore, image processing technology has been used more frequently to analyze and understand ceramic images to assist in ceramic identification and anti-counterfeiting. For example, Wang and others [5] have found that embedding watermarks in the design stage of flower paper has a certain anti-counterfeiting effect on ceramics. In the application of anti-counterfeiting technology to art ceramics, Yuan and others [6] have summarized the feasibility of nondestructive testing techniques such as optical microscopy imaging and CT scanning. With the rapid development of artificial intelligence technology, many scholars have started to combine artificial intelligence and image processing technology with ceramic recognition and anti-counterfeiting. For instance, Mu [7] and others have studied AI-aided recognition of ancient ceramics, consequently, machines instead of experts, can intuitively recognize ancient ceramics. Yang [8] has proposed a feature extraction and classification algorithm for ceramic surface images based on artificial neural networks and extracted shape features for separated surface defects.

Based on the above analysis, combining image processing algorithms and artificial neural networks for ceramic identification is feasible both in theory and in practice. However, most image processing algorithms are aimed at macroscopic parameters such as the shape, size of ceramics, and patterns to determine the “identity identification” of art ceramics. It becomes more and more difficult for these methods to deal with the continuous refinement of imitation art ceramics counterfeits on the market. In addition, these methods generally require particular devices to collect required ceramic information, such as infrared spectrometer [9], X-CT [10] and so on. However, these devices are usually large, complex, expensive, and cumbersome to be applied on a large scale. Therefore, it is vital to find a new method to identify ceramics. The firing process of ceramics is physical and chemical. Even if the raw materials are the same, the firing conditions will change slightly [11]. For instance, the type of the vessel, the holding time, and other factors will lead to changes in the microstructure of the art ceramics in a specific region, such as the formation of microcracks, bubbles, and characteristic crystals. In such a region, the combination of random structural features is difficult to repeat during the preparation process. Furthermore, these structural features are unaffected by corrosion and wear. Therefore, this paper proposes to selected the unique microstructure feature to carry out testing and comparative tracing due to its non-repeatability and good stability. However, compared with the general images, the microscopic images have a large number of irregular features which have increased the difficulty of feature extraction, and thus it is more difficult to collect samples. Although deep learning has already been widely used in image matching [12]. It is difficult to apply the deep learning methods to identify ceramic microcosmic images because of the above problems. On the contrary, due to high robustness and the need for a small number of data samples, SURF and other traditional algorithms based on the manual is more suitable for processing these images in practical applications. Especially in detecting the feature points, the traditional detection methods can detect very stable and consistent feature points under different lighting, scale, and rotation changes [13].

In this paper, the several common feature extraction algorithms have been compared.These are scale invariant feature transform (SIFT) algorithm [14], speed-ed up robust features (SURF) algorithm [15], oriented FAST and rotated BRIEF (ORB) algorithm [16], and binary robust invariant scalable keypoints (BRISK) algorithm [17]. Due to higher accuracy requirements, the SURF algorithm has been adopted to extract irregular features of ceramic local microscopic images [18]. The random sample consensus (RANSAC) method has been simultaneously used to remove unreliable matching point pairs [19]. The SURF features obtained by the above algorithms are used as the unique identification of the ceramic and then stored in the unique identification database. The traditional centralized storage is not so safe and reliable. Because of the immutability of blockchain technology, storing images and extracted features on the blockchain have greater credibility.

However, the capacity and rate of data storage in traditional blockchain systems are so low that they cannot store large-scale data. Based on this consideration, the “blockchain + distributed storage” is used to solve the problem of large-scale data storage. Firstly, the interplanetary file system (IPFS) [20] has distributed storage of photographed ceramic microscopic image features and generated the unique corresponding hash as the unique

identifier for this ceramic, then establishing a database to store hash data on the blockchain. Hyperledger Fabric [21] as open-source blockchain technology can be used to store these data. At the same time, the circulation record and comparison record of the ceramic can be queried to judge the degree of concern about the ceramic. At any time, the authenticity of the art ceramic can be determined by comparing images with the feature point sets of those images stored on the blockchain, thus achieving the anti-counterfeiting of modern art ceramics in technology.

The method proposed in this paper can replace experienced experts and particular expensive devices. The cost of the required device for the proposed method is about 10% price of those particular expensive devices. The speed of obtaining identification results is also greatly improved compared to the previous methods. It does not need to add any information labels to ceramics. In addition, the unrepeatable microscopic characteristics of ceramics are used as the only identification of ceramics. The microscopic features are extracted using the " SURF+RANSAC " algorithm. These features are stored on the blockchain to ensure the unforgeability of ceramics and reliability of identification results.

2 Proposed Recognition Method of Ceramic Microcosmic Images

2.1 SURF Feature Extraction

The Speeded-up Robust Feature (SURF) is a Robust local feature point detection and description algorithm. The SURF algorithm can be seen as the improved algorithm of the SIFT algorithm. The SURF operator maintains the excellent performance characteristics of SIFT operator. It also offsets the disadvantages of SIFT, such as high computational complexity and time-consuming performance. In addition, it improves the computational speed and the execution efficiency, making it more conducive to extracting features and descriptions of ceramic microcosmic images efficiently in the general computer.

(1) Constructing scale-space

Firstly, the scale-space needs to be divided into several groups. Each group, in turn, consists of several fixed layers. The same set of images with different layers uses the same size filter, but the filter's scale-space factor (the Gaussian blur coefficient σ) gradually increases. When constructing a scale-space, for an image f(x, y), its Hessian matrix is calculated based on (1).

$$H(f(x,y)=\begin{bmatrix}\frac{\partial^2 f}{\partial x^2}\frac{\partial^2 f}{\partial x\partial y}\\ \frac{\partial^2 f}{\partial x\partial y}\frac{\partial^2 f}{\partial y^2}\end{bmatrix}. \tag{1}$$

However, Gaussian filtering is required for the image before constructing the Hessian matrix. After filtering, the Hessian matrix of a certain point F in the image f on the scale of σ can be expressed as (2).

$$H\left(F,\sigma\right)=\begin{bmatrix}L_{xx}(F,\sigma)L_{xy}(F,\sigma)\\ L_{xy}(F,\sigma)L_{yy}(F,\sigma)\end{bmatrix}. \tag{2}$$

n these equations, $L_{xx}(F, \sigma)$, $L_{yy}(F, \sigma)$, $L_{xy}(F, \sigma)$ respectively represents gaussian second-order partial derivative , $\frac{\partial^2 f}{\partial x^2}$, $\frac{\partial^2 f}{\partial y^2}$ and $\frac{\partial^2 f}{\partial x\partial y}$ convolution with image f at F. When the discriminant of the Hessian matrix obtains a local maximum, the current point can be considered as a point that is brighter or darker than other points in the surrounding neighborhood, thus determining this point as the key point and locating its position.

Since the Gaussian kernel is normally distributed, the coefficient becomes lower and lower from the center point outward. In order to improve the operation speed of the Gaussian convolution, SURF uses a box filter to approximate the Gaussian filter. The result of convolution between the box filter and the image is represented by D_{xx}, D_{xy}, D_{yy}, which are used to replace L_{xx}, L_{xy}, L_{yy} in order to get an approximation of the Hessian matrix H whose row column is as shown in equation (3). Multiply D_{xy} by a weighting factor of 0.9 to balance the error caused by the use of a box filter approximation:

$$\det(H) = D_{xx} * D_{yy} - (0.9 * D_{xy})^2. \quad \textbf{(3)}$$

Fig. 1 below shows the box filter that transforms the image filtering into the calculation of the addition and subtraction of pixels between different regions of the image, which is the strong point of the integral graph. All they need to do is to search the integral graph simply a few times, then the speed of constructing scale-space will be greatly increased.

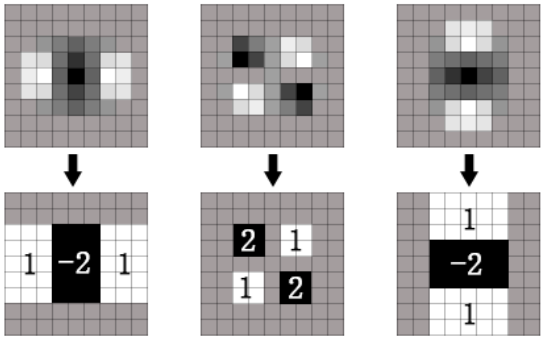

Fig. 1. The box filter

(The upper three figures are the corresponding second derivatives values of the 9*9 Gaussian filter template in the vertical direction of the image respectively. The lower three figures are approximated by the cassette filter. The pixel value of the gray part is 0, the black is -2, and the white is 1.)

(2) Filtering and positioning feature points

Find the local maximum of the scale-space, then filter out the key points with a weak response or the ones with error location, and finally screen out the final stable feature points.

(3) Confirming feature points direction

In the circular neighborhood of the feature points, count the sum of the horizontal and vertical Haar wavelet features of all points in the 60-degree sector. Then the sector should be separated by 0.2 radians after performing a rotation and counting the harr wavelet eigenvalues in the area again. Finally, the direction of the sector with the largest value will be taken as the main direction of the feature point.

(4) Generating feature point description vectors

In this part, a 4*4 rectangular area block around the feature point is set along the main direction of the feature point. Each sub-region counts the Haar wavelet characteristics of 25 pixels in both the horizontal and vertical directions, where both the horizontal and vertical directions are relative to the main direction. The Haar wavelets are characterized by the sum of the horizontal values, the vertical values, the horizontal absolutes, and the sum of the absolute vertical values. This process is as shown in Fig. 2. In this way, SURF extracts a 4*4*4 64-dimensional feature vector.

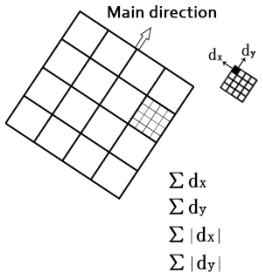

Fig. 2. Schematic diagram of feature vectors extraction with SURF

2.2 RANSAC Feature Filtering

The random sample consensus (RANSAC) algorithm is an indeterminate algorithm. By improving the iteration times of the algorithm, there is a certain probability of obtaining a more reasonable result. It can iteratively estimate the parameters of a mathematical model from a set of observations containing the "outlier point".

RANSAC algorithm assumes that the data consist of "interior-points", and the distribution of the data can be explained by some model parameters [22]. The extreme values of noise, incorrect measurement methods, and incorrect assumptions about the data may produce "outlier-points". The "outlier-points" are the data that cannot fit the model. The remain data points other than "outlier-point" and "interior-points" will be considered noise. This model can interpret or apply to the "interior-points". The matching relationship between the query image and the target image in the image matching process can be described by a basic matrix that can represent the correspondence between points and points, as shown in (4) and (5).

$$x_2^T F x_1 = 0. \tag{4}$$

$$\begin{bmatrix} x_2 y_2 1 \end{bmatrix} \begin{bmatrix} f_{11} f_{12} f_{13} \\ f_{21} f_{22} f_{23} \\ f_{31} f_{32} f_{33} \end{bmatrix} \begin{bmatrix} x_1 \\ y_1 \\ 1 \end{bmatrix} = 0, \tag{5}$$

where (x_1, y_1) represents the point of the query image, and (x_2, y_2) represents the point of the target image. In this paper, the main process of the RANSAC algorithm in the proposed method is as follows:

Step I: Select a random RANSAC sample from the microscopic ceramic image sample set.

Step II: Calculate the transformation matrix M based on these matching point pairs.

Step III: Calculate the consistent set satisfying the current transformation matrix according to the sample set, transformation matrix M, and error measure function, and return the number of elements in the consistent set.

Step IV: Determine whether it is the optimal or maximum consistent set according to the number of elements in the current consistent set. If it is, the current optimal consistent set is updated.

Step V: Update the current error probability P. If P is greater than the minimum allowable error probability, repeat step I to step IV to continue the iteration until the current error probability P is less than the minimum error probability.

2.3 Data Storage Based on Blockchain

Data storage plays a key role in the traceability chain of ceramic identification. The combination of distributed storage and blockchain can not only ensure the security of data but also ensure the file storage capacity of large-scale data.

The interplanetary file system (IPFS) aims to create a persistent and distributed network transport protocol for storing and sharing files. It is a content-addressable peer-to-peer hypermedia distribution protocol [23]. Nodes in an IPFS network will form a distributed file system. IPFS combines multiple technologies such as Distributed Hash Tables (DHT) system [24], BitTorrent, Git, Self-Certified Filesystems (SFS), and content distribution network protocol with blockchain. It successfully simplifies and combines proven techniques into a single cohesive system greater than the sum of its parts [25]. IPFS can trace the content by generating independent hash values through file content to identify files. The file modification history can also be traced. IPFS should be the most basic architecture system to realize the circulation identification of high-end ceramic art products with blockchain technology. The IPFS system uses a hashing algorithm to ensure that the data cannot be tampered with and to keep the data intact and valid. Meanwhile, it generates a separate ID for each data in the IPFS network. Ceramic identification can rely on the ID to determine the authenticity and validity of data, thus significantly improving the security of this ceramic identification traceability chain.

Hyperledger project founded by Linux Foundation [26] is an open-source, distributed ledger. This project is divided into five subprojects, and the Fabric project is one of them. Hyperledger Fabric is a licensed, distributed ledger platform that is widely used in multiple domains. It uses ledgers, and smart-contracts like other blockchain technologies. Hyperledger Fabric allows participants in alliances to develop and deploy applications by using blockchain. It records all interactions between parties as transactions [27]. All transactions on the network have

to be endorsed. Only the endorsed transactions can be committed to the blockchain and update the global state [28]. However, Hyperledger Fabric is difficult to store large-scale data due to the constraints of storage, computation, and other resources. Therefore, this paper uses blockchain combined with distributed storage to solve the problem of storing large-scale data on the chain [29]. The original data is stored in IPFS first, and the hash addresses of these data are stored on Hyperledger Fabric for permanent preservation. Data can be queried at any time by hash address information stored on the Hyperledger Fabric.

It is of top priority to store numerous microscopic images obtained previously and feature point sets of these images on IPFS and obtain unique hash addresses, and store these hash addresses on Hyperledger Fabric. Query can always be made about these data through the hash address of the file on the blockchain, thus ensuring the security of the data and the reliability of the identification and traceability work. The Fig. 3 shows the main process for storing and querying the feature point sets of ceramic microscopic images. The reason why the feature point sets are also stored is that the subsequent matching process does not necessarily use the complete microscopic images, and using the feature point sets for storage can speed up the time to obtain the feature point pairs.

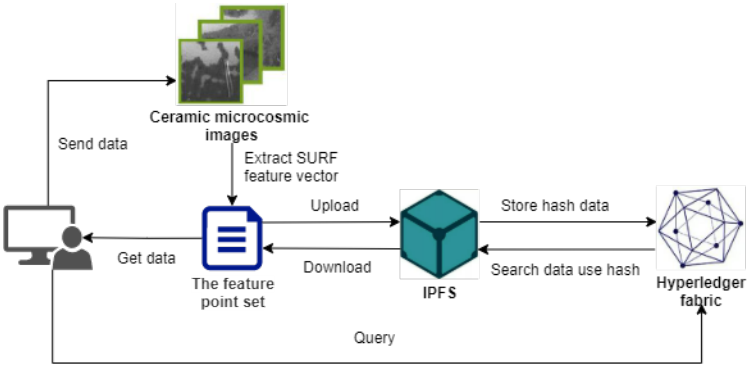

Fig. 3. Store and query the feature point set of ceramic microscopic images

2.4 The Criteria of Matching Evaluation

Since the logarithm of feature points in different pictures is different, it is impossible to judge whether the matching is successful or not simply by judging the logarithms of feature points. Therefore, it is necessary to introduce a matching similarity rate (MSR) as an important indicator to estimate image matching performance. It can be calculated according to (6).

$$MSR = \frac{N_c}{N_c + N_e}. \tag{6}$$

N_c represents the correct number of matching points, N_e represents the number of incorrect matching points, and P represents the percentage of the correct number of matching point pairs in the number of all matching point pairs.

2.5 Identification Workflow of the Proposed Method

The full algorithm flow of proposed ceramics recognition processs is as shown in Fig. 4.

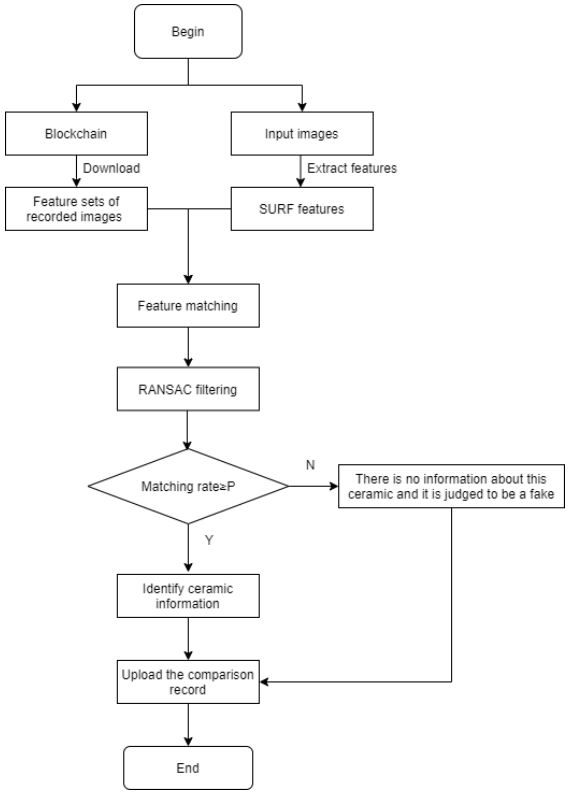

Fig. 4. Flow graph of ceramic identification system

In the matching process, the image is the first input to be matched. And the feature points are extracted quickly by the SURF. Then the SURF feature vector set of the image can be compared with the SURF feature vector set of the registered ceramic microcosmic image stored on the blockchain. In order to improve the matching effort rate, the FLANN algorithm is applied to find the matching point pairs with the nearest distance between the ceramic micro-image to be matched and the approximate ceramic image in the database. Euclidean distance is used to find the nearest neighbor distance. For each feature point in the query image, it is necessary to find the two points closest to the point in the target image. If the ratio of the closest distance to the second distance is less than a certain ratio, the point is considered to be a correct match. Otherwise, it is a falsely matched point, and it should be eliminated. The ratio value generally ranges from 0.6 to 0.8, and 0.8 is used in this paper.

After the initial filtering of feature pairs by the FLANN algorithm, there may still be many incorrect matching points- pairs. These incorrect matches can be extremely disruptive to the final match result. In order to ensure the accuracy of the experimental results, the RANSAC algorithm is used to filter again and eliminate incorrect matches. After obtaining relatively pure feature point pairs, the feature point matching will be done, and the logarithm will be used to sort the resulting set of matching points. The matching similarity rate of the most matching point pairs can be calculated. If the obtained matching similarity rate is greater than the set threshold, it can be considered genuine. Finally, the comparison record should have been stored on the Hyperledger Fabric.

3 Experiments and Analysis

The experimental platform used in this paper is a personal computer with a Windows 10 operating system, configured as an Intel Core i5-1135G CPU, with 16GB of memory. In this paper, it is proposed to select the matching accuracy rate and the running time of the algorithm in the matching process as the evaluation indicators to analyze and evaluate the algorithm.

3.1 Comparison Experiment of Four Algorithms

The matching of feature points is a critical step in image matching. Whether the feature points can be accurately matched has a direct effect on the final image matching. During the firing process, ceramics have physical and chemical properties which are unrepeatable and likely to produce random distribution characteristics like bubbles, as shown in Fig. 5.

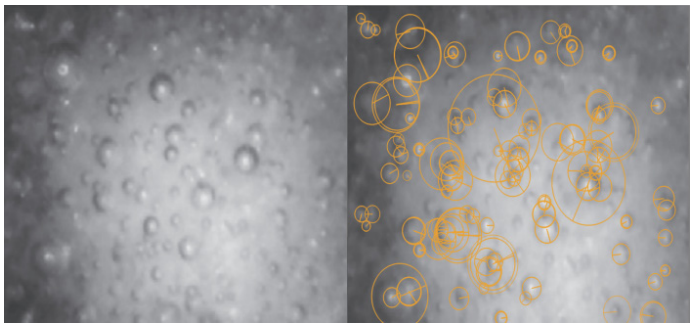

Fig. 5. Irregular bubble characteristics and extracted feature points in ceramic microscopic images

The irregular bubble characteristics of ceramic microscopic images have been used to compare the four commonly used traditional feature selection algorithms: SIRF, SURF, BRISK, and ORB. Several groups of randomly intercepted images of ceramic samples have been selected as the control group to compare the matching effects of the four algorithms. The comparison results are shown in Table 1. It can be seen that the average calculation speed of BRISK is the fastest. And the average calculation speed of ORB is also faster than that of SURF and SIFT. The average calculation speed of SURF is almost the same as that of SIFT. The time gap of these algorithms is not large for the actual identification process. However, the difference in the number of feature points is very obvious in the accuracy of the final result. It is obvious that the number of feature points obtained by SURF is much greater than that of the other three. Because ceramic identification depends on high accuracy, the requirements for real-time performance are not very high. Moreover, the average time taken to obtain the results by SURF is also far less than the manual identification or other identification methods. In addition, rotation, flip, blur, and illumination comparison experiments have been conducted on the four algorithms to simulate various situations that may be encountered during the process of shooting and sampling. It can be seen from the Fig. 6 that in the simulation experiments with rotation, flip, and blur, both SIFT and SURF perform slightly better than BRISK, but far better than ORB. In the experiment of adjusting the brightness, neither BRISK nor ORB performs well. No matter which kind of experiment, the average matching similarity rate of SURF and SIFT are both much higher than that of the other two algorithms. And although SURF is slightly inferior to SIFT in terms of time performance, the robustness performance of SURF is the best among the four algorithms under all the experiments. Therefore, it is concluded that if the real-time requirements of the calculation are very high, the BRISK algorithm can be selected; if the requirements for practicability are slightly higher, and the requirements for accuracy are relatively high, then SURF is a better choice.

Table 1. Comparison of four traditional feature extraction algorithms

Algorithm	Average matches	Average time (in sec)
SIFT	380	0.883
SURF	707	0.964
ORB	297	0.324
BRISK	162	0.248

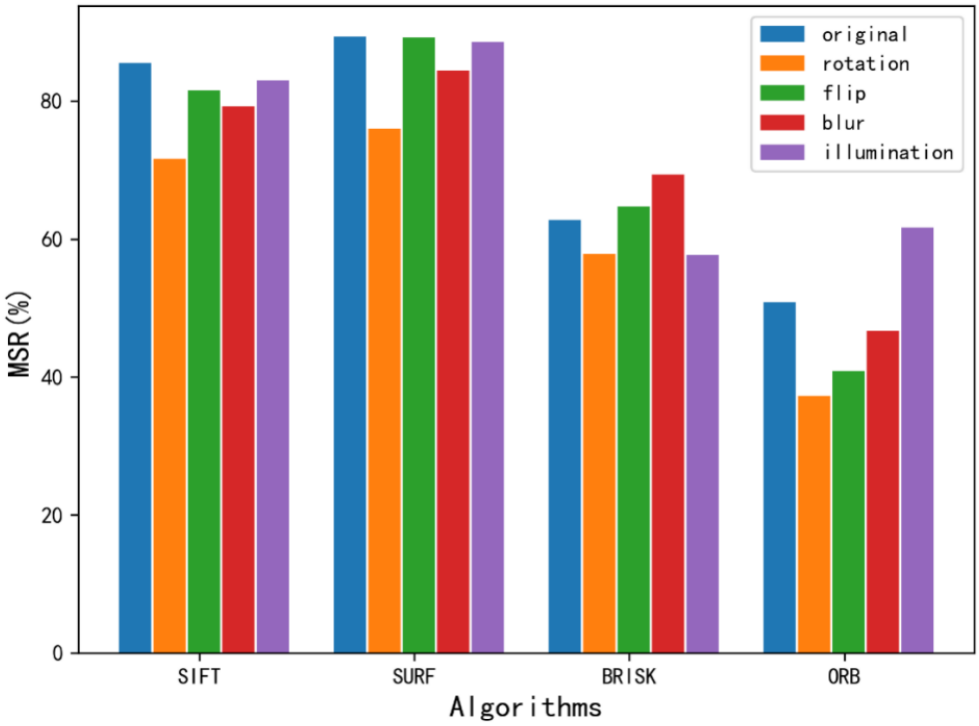

Fig. 6. Matching similarity rate of different algorithms in different conditions

After having compared the four commonly used feature extraction algorithms of SIFT, SURF, ORB, and BRISK. SURF has been finally chosen to extract the irregular features of the ceramic local microscopic image due to the higher accuracy requirements. And it will constitute the local feature vector set of the image. These local feature vector sets are considered unique features of the ceramic. Even if for the modification of rotation, brightness and illumination in the process of taking ceramic microscopic images. Local features can still be correctly extracted so that the authenticity of the ceramics can be effectively discriminated. After the feature selection algorithm has been determined, the selection of different Hessian matrix thresholds will affect the effect of the algorithm. After having compared, this paper chooses 550 as the minimum Hessian matrix threshold.

In the process of SURF feature point matching SURF, there will be many incorrect matching point pairs which usually look like some staggered lines in the matching results. When these mismatched point pairs account for a high proportion of the obtained matching point set. Not only will the running time slow down, but also the final matching result will be greatly impacted. Therefore, a better method is needed to eliminate these incorrect matching points. RANSAC algorithm can calculate the model parameters according to a set of correct data. It is undoubtedly suitable for filtering incorrect points. Therefore, RANSAC is used to eliminate incorrect matching points to obtain a better matching effect. Although SURF can filter some incorrect matching points through FLANN filtering, there are still some incorrect matching items according to the comparison. The higher the error rate for matching, the more intersections will be formed.

Although pure SURF can also complete target matching, when the number of incorrect matching points increases, the matching accuracy will be very low or be failed. The combination of SURF+RANSAC has been adopted, which can effectively eliminate the incorrect matching points on the basis of ensuring the number of matching feature points. The Fig. 7 shows that the matching results between different feature points of the same image use SURF and SURF + RANSAC respectively. It is obvious that the introduction of the RANSAC algorithm can obviously filter some wrong matching points, such as the matching item with a large deviation at the bottom of the image (a).

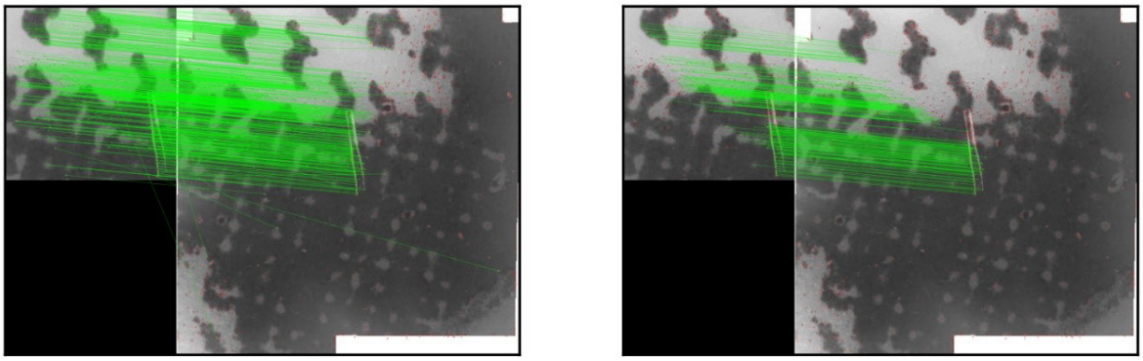

(a) SURF (b) SURF+RANSAC

Fig. 7. The feature matching of an image with its sheared image using

As shown in Table 2, the introduction of the RANSAC algorithm can improve the matching similarity rate of the overall feature points almost by 8%. An appropriate distance has been selected for the SURF + RANSAC algorithm. Through the setting of distance, the number of matching point pairs has been reduced. But the correct matching similarity rate has been improved after filtering out the wrong matching point pairs. The proposed algorithm makes the overall correct matching similarity rate to be the highest. Since the anti-counterfeiting and traceability of ceramics stress more on accuracy rather than timeliness, it is very worthwhile to sacrifice a little time cost to obtain higher accuracy. Although its matching time would increase compared with the pure surf algorithm, its matching accuracy is improved, the stability of the algorithm is improved, and the real-time performance of the algorithm will not be affected so much. Experimental results show that the proposed algorithm can not only improve the quality of matching point pairs and the matching accuracy but also generate excellent robustness under a variety of image changes. Although there may still be some wrong matching points after filtering by RANSAC, it still plays an important role in eliminating the robustness and optimizing the algorithm to improve the matching accuracy and makes the matching of ceramic microcosmic images more stable and more possible to succeed.

Table 2. Comparison by different methods

Algorithm	Total matches	Right matches	Error matches	MSR (%)	Time (in sec)
SIFT	383	315	68	82.24	0.883
SURF	423	487	64	86.85	0.964
SIFT+RANSAC	157	142	15	90.44	1.236
Proposed	138	129	9	93.47	1.437

3.2 Experiments on Ceramic Microscopic Image Datasets

In order to verify the efficiency of the proposed algorithm more intuitively, 20 sample sets of ceramic microscopic image dataset have been selected. Each group has 100 different microscopic images of the same ceramic. The 100 images in each set have different rotation angles and sizes for the simulation of the possible position offset, and the angle changes during the multiple microscopic images shot of the same position. Many experiments have also been carried out on matching similar images randomly. The Fig. 8 shows the results of one experiment that the highest matching similarity rate of these samples can reach 90%, while the second-highest matching similarity rate reaches only 12.02%. The lowest matching similarity rate is only 1.92%. It is fully proved that the proposed algorithm can find the ceramic corresponding to the image to be compared in many microcosmic images with similar structural characteristics.

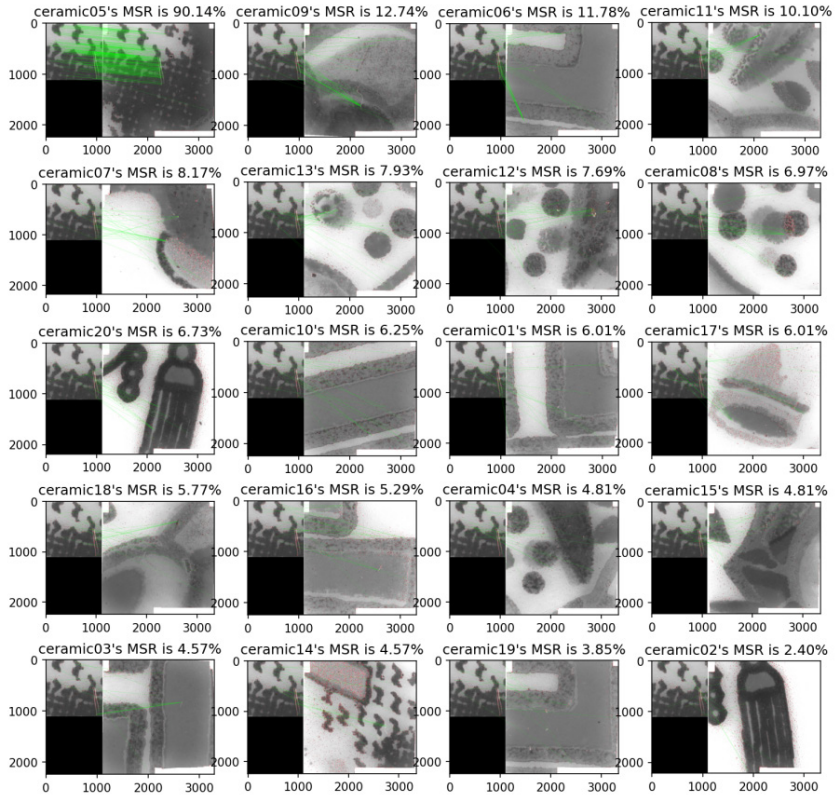

Fig. 8. Random choose 1 image from 20 groups of similar microscopic images for comparison

In addition, more data samples have been used for testing to verify the authenticity and reliability of this conclusion. Ten groups of samples have been randomly selected, and ten microscopic images have been randomly selected with different positions and different angles in each group as the matching group of the experiment. At the same time, ten images that did not belong to the original sample have been selected for multiple experiments so as to simulate the process of matching the newly captured microscopic ceramic image with the stored microscopic ceramic image in practical application. It is likely to test whether the proposed algorithm can be used to select the correct matching image in the matching. Although some of the images represent a high similarity to the naked eye, this algorithm can calculate their similarity very well. As shown in Table 3, in addition to the similarity of the correctly matched group that reaches more than 90%, the similarity of other comparison groups reaches less than 15%, and the difference is very obvious. The average matching similarity of each group of similar images is maintained at about 1% to 15%, which is far from the standard threshold of correct matching. The results of many other experiments are similar to this conclusion, so it is concluded that the proposed method can correctly find the expected microscopic image of the ceramic in many similar images.

Table 3. Matching result of 10 images with 10 templates

MSR (%)	T_1	T_2	T_3	T_4	T_5	T_6	T_7	T_8	T_9	T_{10}
i_1	**88.92**	6.52	1.92	0	3.17	7.54	0	2.38	4.52	12.32
i_2	1.21	**91.54**	0	3.17	7.64	2.76	1.52	4.05	9.86	6.18
i_3	2.66	3.19	**87.63**	1.32	4.13	2.25	1.73	3.63	1.18	4.70
i_4	3.56	8.52	7.14	**86.07**	8.48	5.78	4.89	9.82	1.18	3.03
i_5	0	7.57	8.33	2.55	**90.58**	7.14	3.63	2.68	11.11	1.50
i_6	13.76	7.12	12.50	4.55	4.58	**81.81**	5.55	2.94	3.12	0
i_7	2.17	1.78	1.72	4.00	8.82	4.55	**86.00**	0	6.81	1.69
i_8	5.41	5.56	12.57	4.27	4.46	3.47	2.67	**93.63**	0	1.52
i_9	6.73	1.85	8.15	5.85	1.34	2.63	1.33	0	**83.17**	6.89
i_{10}	1.81	11.65	6.25	6.84	7.15	5.20	3.56	4.46	10.52	**85.75**

Experimental results show that, by comparing between the image to be compared and the image dataset of existing ceramic microscopic, it can be accurately judged whether the ceramic is fake or not. The contrast between most fakes and genuine products will not exceed 15%. Even if it exceeded 15%, it would be so difficult for it to exceed 60% that the ceramics can be identified as imitations. Thus it can be concluded that the ceramic image can be identified quickly and efficiently by the proposed algorithm.

3.3 Experiments on Similar Image Datasets

The proposed method has a good performance on ceramic microscopic image datasets through previous experiments. Although ceramic microscopic images have their own uniqueness due to the randomness of bubbles, there are still some similar microscopic images that are more difficult to distinguish with the naked eye. For example, The Fig. 9 shows an example of the ceramic microscopic image used in this paper and the high-resolution transmission electron micrographs of the dual drug [30]. Both them were found to have several spherical shapes, and some of the small black dots on Fig. 9(b) are more likely to be mistaken for bubbles. These similarities have the potential to influence the final identification results.

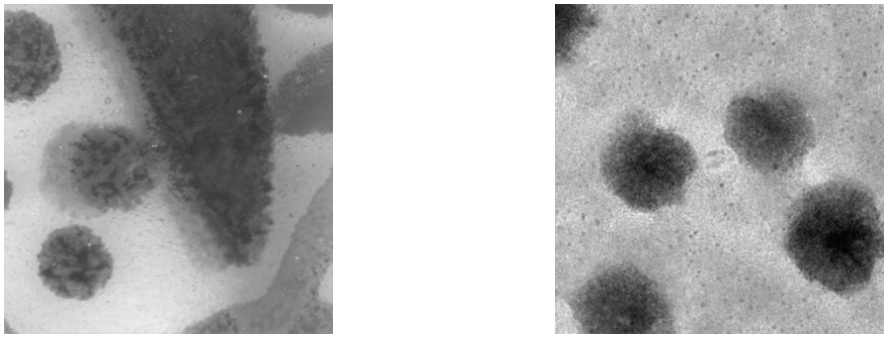

(a) An example of ceramic microscopic images (b) Dual drug loaded PEGylated liposomes

Fig. 9. Similar images

In order to verify the reliability of the proposed algorithm, 20 groups of similar microscopic image sets were selected to experiment. These images have similar microscopic features with our samples. Each image was selected from these 20 groups to match with all the ceramic microscopic images set. The Fig. 10 shows the results on experimental results for three of the samples. The results shows that the average matching similarity rate between sample images and microscopic image sets is around 2%-12%, and the highest matching similarity rate will not be higher than 15%. In addition, the overall experimental results are generally consistent with this conclusion. The above experiments prove that the proposed algorithm can distinguish these microscopic feature images that look very similar to ceramic microscopic images effectively.

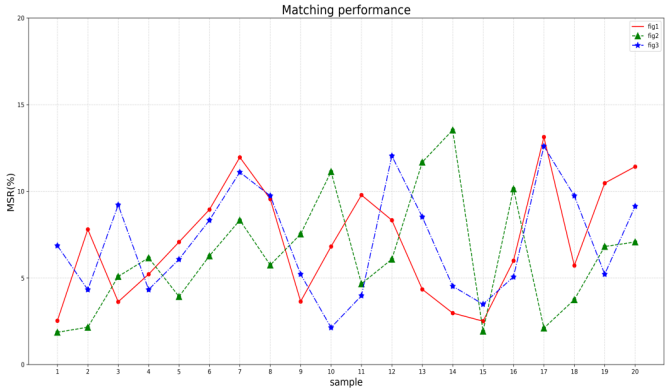

Fig. 10. Results obtained by randomly selecting 3 sample images to match with 20 sets of similar microscopic images

4 Conclusion

Given that there are still some problems in existing traditional methods for the identification and anti-counterfeiting of high-value artistic ceramics, such as time-consuming identification and unguaranteed reliability. In order to solve the above problems, a more rapid and efficient identification method has been proposed without destroying the integrity of ceramics by using the random features of ceramic microscopic images combined with computer vision. Experimental results show that by comparing the captured image features with the preserved microscopic image features, the authenticity and identity of the ceramic can be quickly judged. The proposed method can be used for the identification and anti-counterfeiting of ceramics and can be applied to the identification work in other industries. For example, it can be used to examine the microscopic characteristics of the cap mouth of expensive alcoholic beverages to see if there are traces of secondary packaging, thus avoiding "the useless reformation of the old suffusing old bottles for the new wine." Due to the higher value of art ceramics, the distributed storage combined with blockchain technology can make the identification more secure and reliable than the traditional form of storing ceramic image data. However, the proposed method still needs some improvements. Since ceramic microscopic images have certain requirements on sampling positions. The accuracy of anchoring points is required when taking sampling images. Future work will focus on how to improve the accuracy and efficiency of anchoring, and try to combine deep learning algorithms to identify bubble characteristics to make the system adaptable to more complex recognition environments. In conclusion, the SURF algorithm combined with blockchain technology for ceramic microscopic image identification is a promising method for the anti-counterfeiting traceability of ceramics.

Acknowledgment

This work was supported by the Natural Science Foundation of Fujian Province of China (No. 2021J011007), the Natural Science Foundation Project of Zhangzhou (ZZ2020J24), Principal's Foundation of Minnan Normal University (KJ19015), the Program for the Introduction of High-Level Talent of Zhangzhou and the National Natural Science Foundation of China (No. 61702239).

References

[1] W.-M. Li, Research on methodology of ceramic identification theory, China Cultural Heritage Scientific Research (1) (2011) 60-62.
[2] C.-Y. Dai, F. Du, The methods of ancient ceramics identification, Shandong Ceramics 28(3)(2005) 40-43.
[3] R. Weinstein, RFID: a technical overview and its application to the enterprise, It Professional 7(3)(2005) 27-33.
[4] A. Babor, T. Bjorninen, V.A. Bhagavati, L. Sydänheimo, P. Kallio, L. Ukkonen, Small and flexible metal mountable passive UHF RFID tag on high-dielectric polymer-ceramic composite substrate, IEEE Antennas and Wireless Propagation Letters (11)(2012) 1319-1322.
[5] J.-X. Wang, B. Yang, Y.-H. Zhu, Study on anti-counterfeiting decal making technique based on watermarking algorithm, Journal of Ceramics 32(1)(2011) 87-90.
[6] W.-Z. Yuan, T. Fang, Q.-B. Chang, Y.-Q. Wang, Y. Wu, Application of stereomicroscopes technology in the anti-counterfeiting and identification for modern ceramic art, China Ceramics 32(1)(2012) 31-33.
[7] T.-H. Mu, F. Wang, X.-F. Wang, H.-J. Luo, Research on ancient ceramic identification by artificial intelligence, Ceramics International 45(14)(2019) 18140-18146.
[8] L.-Q. Yang, Ceramic surface image feature extracting and classifying algorithms based on artificial neural networks, in: Proc. 2014 International Conference on Intelligent Systems Design and Engineering Applications, 2014.
[9] X.-P. Wu, Y.-P. Guan, W.-D. Li, H.-J. Luo, Visible-near infrared spectroscopy based chronological classification and identification of ancient ceramic, Spectroscopy and Spectral Analysis 39(3)(2019) 756-764.
[10] W.-Z. Yuan, T. Fang, Q.-B. Chang, G.-S. Li, D. Yu, Application of X-CT technology in the ceramic art anti-counterfeiting and identification, China Ceramics 48(7)(2012) 34-38.
[11] W.-Z. Yuan, H.-X. Zhang, F. Li, P.-F. Jiang, T. Fang, T. Ye, Study on the inspection and verification of ceramic art works based on the characteristics of materials, China Ceramics 51(11)(2015) 57-62.
[12] X.-Y. Jiang, J.-Y. Ma, G.-B. Xiao, Z.-F. Shao, X.-J. Guo, A review of multimodal image matching: methods and applications, Information Fusion 73(2021) 22-71.
[13] S.A.K. Tareen, Z. Saleem, A comparative analysis of sift, surf, kaze, akaze, orb, and brisk, in: Proc. 2018 International Conference on Computing, Mathematics and Engineering Technologies, 2018.

[14] P.C. Ng, S. Henikoff, SIFT: Predicting amino acid changes that affect protein function, Nucleic Acids Research 31(13)(2003) 3812-3814.
[15] H. Bay, A. Ess, T. Tuytelaars, L.V. Gool, Speeded-up robust features (SURF), Computer Vision and Image Understanding 110(3)(2008) 346-359.
[16] E. Rublee, V. Rabaud, K. Konolige, G. Bradski, ORB: An efficient alternative to SIFT or SURF, in Proc. 2011 International Conference on Computer Vision, 2011.
[17] S. Leutenegger, M. Chli, R.Y. Siegwart, BRISK: Binary robust invariant scalable keypoints, in: Proc. 2011 International Conference on Computer Vision, 2011.
[18] J. Zhao, Sports motion feature extraction and recognition based on a modified histogram of oriented gradients with speeded up robust features, Journal of Computers 33(1)(2022) 63-70.
[19] O. Chum, J. Matas, Optimal randomized RANSAC, IEEE Transactions on Pattern Analysis and Machine Intelligence 30(8)(2008) 1472-1482.
[20] M. Naz, F.A. Al-zahrani, R. Khalid, N. Javaid, A.M. Qamar, M.K. Afzal, M. Shafiq, A secure data sharing platform using blockchain and interplanetary file system, Sustainability 11(24)(2019) 7054.
[21] P. Thakkar, S. Nathan, B. Viswanathan, Performance benchmarking and optimizing hyperledger fabric blockchain platform, in: Proc. 2018 IEEE International Symposium on Modeling, Analysis, and Simulation of Computer and Telecommunication Systems, 2018.
[22] K.G. Derpanis, Overview of the RANSAC algorithm, Image Rochester NY 4(1)(2010) 2-3.
[23] S. Muralidharan, H. Ko, An InterPlanetary file system (IPFS) based IoT framework, in: Proc. 2019 IEEE International Conference on Consumer Electronics, 2019.
[24] S. Rhea, B. Godfrey, B. Karp, J. Kubiatowicz, S. Ratnasamy, S. Shenker, H. Yu, OpenDHT: a public DHT service and its uses, in: Proc. 2015 Conference on Applications, Technologies, Architectures, and Protocols for Computer Communications, 2015.
[25] C.Patsakis, F. Casino, Hydras and IPFS: a decentralised playground for malware, International Journal of Information Security 18(6)(2019) 787-799.
[26] X.-Q. Xu, G. Sun, L. Luo, H.-L. Cao, H.-F. Yu, A.V. Vasilakos, Latency performance modeling and analysis for hyperledger fabric blockchain network, Information Processing & Management 58(1)(2021) 102436.
[27] E. Androulaki, A. Barger, V. Bortnikov, C. Cachin, K. Christidis, A.D. Caro, D. Enyeart, C. Ferris, G. Laventman, Y. Manevich, S. Muralidharan, C. Murthy, B. Nguyen, M. Sethi, G. Singh, K. Smith, A. Sorniotti, C. Stathakopoulou, M. Vukolic, S.W. Cocco, J. Yelick, Hyperledger fabric: a distributed operating system for permissioned blockchains, in: Proc. 2018 EuroSys Conference, 2018.
[28] M.S. Ali, M. Vecchio, M. Pincheira, K. Dolui, F. Antonelli, M.H. Rehmani, Applications of blockchains in the Internet of Things: A comprehensive survey, IEEE Communications Surveys & Tutorials 21(2)(2018) 1676-1717.
[29] Z. Meng, T. Morizumi, S. Miyata, H. Kinoshita, Design scheme of copyright management system based on digital watermarking and blockchain, in: Proc. 2018 IEEE Annual International Computer Software and Applications Conference, 2018.
[30] A. Mohan, S. Narayanan, S. Sethuraman, U.M. Krishnan, Novel resveratrol and 5-fluorouracil coencapsulated in PEGylated nanoliposomes improve chemotherapeutic efficacy of combination against head and neck squamous cell carcinoma, BioMed Research International, 2014(424239)(2014) 1-14.